



## Hydroxylamine-O-sulfonic Solid acid as an Efficient Anti-hemolytic Catalyst

ZINAB KHADIM RAHEEM<sup>1</sup>, MUNA HASSON SAOUDI<sup>1</sup> and KASIM MOHAMMED HELLO<sup>1\*</sup>

<sup>1</sup>Department of Chemistry, College of Science, Al-Muthanna University, Al-Muthanna Governorate, Samawa, Iraq.

\*Corresponding author E-mail: kasimhello@gmail.com; kasimhillo@mu.edu.iq

<http://dx.doi.org/10.13005/ojc/410425>

(Received: June 08, 2025; Accepted: July 06, 2025)

### ABSTRACT

Si@OSA-Dir and Si@OSA-Ref were produced by immobilization of immobilizing hydroxylamine-O-sulfonic acid (OSA) on rice husk ash in two different ways. The presence of Carbon, Sulfur, and Nitrogen in the silica was verified by elemental analysis. The specific surface area of both catalysts was 257 m<sup>2</sup>/g. The produced catalysts were shown to be stable at temperatures as high as 200°C. The catalysts' cytotoxicity effects, antioxidant potency, and anti-hemolytic activity were evaluated in order to appraise evaluate their biological and medical applications. In contrast to the positive control (H<sub>2</sub>O<sub>2</sub>), which generated a high percentage of hemolysis, the results demonstrated that both catalysts exhibited low hemolytic activity at low concentrations of 100–150 µg/mL. Both catalysts exhibited strong antiradical activity and a generally high H<sub>2</sub>O<sub>2</sub> scavenging activity percentage. The LDH assay demonstrated these catalysts safety and protective properties qualities. When erythrocytes treated with these two catalysts are exposed to hydrogen peroxide, the results are decreased to marginally reduced (554 U/L). These encouraging outcomes for both catalysts by enhancing antioxidant defenses, and scavenging harmful molecules shows promise in improving the efficacy to stabilize and stop the breakdown of red blood cells.

Keywords: Antioxidant, Hemolysis, Rice husk ash, Hydroxylamine-O-sulfonic acid, Soil-gel.

### INTRODUCTION

Silica can be derived from various sources, and one significant source is rice husk waste, which contains over 94% silica and is highly pure<sup>1</sup>. Silica can interact with other organic or inorganic compounds to create new types of "hydride silica-ligand materials. It possesses excellent physical and chemical properties, such as thermal stability, the ability to be modified with other materials, and resistance to microbial attack<sup>2,3</sup>. These characteristics have

attracted the attention of numerous scholars<sup>4,5</sup>.

Silica can be extracted from waste materials and modified with ligands using various methods. One efficient technique is the sol-gel method, which allows for the modification of silica with 3-(chloropropyl)triethoxysilane (CPTES) and organic ligands in a single-pot synthesis that takes only a short time<sup>6</sup>. It has been reported that this modification relies on the formation of a sodium silicate-CPTES complex, which is then converted



into silica with Si-(CH<sub>2</sub>)<sub>2</sub>CH<sub>2</sub>Cl end groups, known as RHACCI. This type of modification enables the easy replacement of chlorine with organic ligands through in-situ transformation, facilitating the creation of heterogeneous catalysts<sup>7,8</sup>. Traditional methods of silica modification with organic ligands typically use harsh solvents, result in low yields, require long reaction times, and involve multiple steps. In contrast, the new methods developed by our team allow for a completely homogeneous procedure<sup>6</sup>. This means that all reactants can interact on the same surface. The advantages of this direct modification include higher yields, shorter preparation times, and the use of environmentally friendly solvents.

Cytotoxicity studies are crucial for characterizing novel compounds or materials that are intended to interact with human biological systems *in vivo*. One of the primary evaluations in these cytotoxicity assessments is to determine how much a compound disrupts the membrane of erythrocytes (red blood cells), which leads to the release of cellular contents. The hemolysis assay is a commonly used method that offers several advantages, including affordability, easy accessibility, and simplicity in execution. When a chemical induces hemolysis, hemoglobin and various cellular components are released into the supernatant. Because hemoglobin has a unique absorption spectrum, a spectrophotometer or plate reader can be employed to measure optical density (OD) values, which helps determine the extent of hemolysis<sup>9,10,11</sup>.

Given the significance of silica-based nanomaterials in biomedical applications, this research highlights their novel and diverse uses, particularly regarding hemolytic effects on human erythrocytes. The cytotoxicity of the prepared catalysts was also evaluated, and their ability to protect red blood cells from damage was reported.

## EXPERIMENTAL

### Raw materials

All chemicals were used directly without further purification. The following were purchased from System: sodium hydroxide (99%) and nitric acid (65%). The following chemicals were acquired from Sigma: CPTES (99%), 1,1-diphenyl-2-picrylhydrazyl radical, acetone (98%), and hydroxylamine-O-sulfonic acid (99.99%). Toluene (98%), methanol,

and ethanol (98% and 100%, respectively) were sourced from GCC. Chloroform (99.4%), ascorbic acid, and hydrogen peroxide (30%) were supplied by Scharlau. Rice husk (RH) was collected from a rice mill in Samawa, Iraq.

### Samples characterizations

The X-ray diffraction pattern was obtained using the Stoe Study-MP diffractometer system. Thermal analyses, including TGA and DTA, were conducted with a Rheometric Scientific System. A nitrogen adsorption analysis was performed using a Nova 2000 Quantachrome analyzer. Scanning electron microscopy combined with energy dispersive X-ray spectroscopy (SEM-EDX) was carried out using a Philips XL30 system. The transmission electron microscopy (TEM) micrograph was obtained using Philips CM12 equipment.

### Silica extraction and modification by reflux method

Amorphous silica was extracted from rice husk ash (RHA) as described in references<sup>12,13</sup>. The ash, which contains 95% silica, was converted into silica with a 3-chloropropyl end group (RHACCI) using a previously reported method<sup>6</sup>. Next, the silica-3-chloropropyl end group was transformed into silica propyl-3-hydroxylamine-O-sulfonic acid (OSA) (referred to as Si@OSA-ref) by adding 1.5 g of OSA in dry toluene to 1.5 g of RHACCI. The mixture was refluxed at 110°C for 48 hours. The expected product, Si@OSA-ref, was isolated through simple filtration, and 50 mL of ethanol was used to wash the product. In the end, finally 1.3 g of Si@OSA-ref was collected and stored for further applications.

### The direct synthesis method of Si@OSA-Dir

First, 3.0 g of ash (silica) was converted to sodium silicate by dissolving it in 100 mL of 1.0 M NaOH while stirring for 30 minutes. In the second step of process, approximately 2.81 g (2.48 mmol) of (OSA) and 6.0 mL of (CPTES) were added. The mixture was then titrated with a 3.0 M nitric acid solution. A gel began to form at a pH of 10.0, and the reaction was terminated at a pH of 3.0. The mixture was left at room temperature for 24 h to allow for aging, after which the gel was isolated by centrifugation (repeated six times for purification). Approximately 5.30 g of Si@OSA-Dir was collected and dried at 110°C.

### Hydrogen peroxides radical scavenging activity

The hydrogen peroxide scavenging activity

was measured using the method described in reference<sup>14</sup>. A total of 100  $\mu\text{L}$  of the test sample was added to a 200 mM hydrogen peroxide ( $\text{H}_2\text{O}_2$ ) solution prepared in a 50 mM phosphate buffer with a pH of 7.4. The mixture was incubated at 25°C for 30 minutes. The remaining unreacted  $\text{H}_2\text{O}_2$  was quantified by measuring the absorbance at 230 nm, using a blank solution that contained only the phosphate buffer without hydrogen peroxide<sup>14</sup>. The ability of the sample to scavenge hydrogen peroxide is estimated as follows:

$$\text{Quenching capacity (\%)} = \frac{A_{\text{Control}} - A_{\text{Sample}}}{A_{\text{Control}}} \times 100$$

#### Anti-Hemolytic activity

The hemolytic activity of Si@OSA-Dir was evaluated by using hydrogen peroxide ( $\text{H}_2\text{O}_2$ ) to induce damage to the membranes of red blood cells (RBCs), following the assay developed by<sup>15,16</sup>. Blood samples were collected from healthy human volunteers, with 5 mL of blood drawn into blood tubes containing EDTA. The erythrocyte suspension was washed three times with a phosphate-buffered saline (PBS) solution. Various concentrations of Si@OSA-Dir were added to the diluted PBS. The reaction mixtures were incubated for 5 min at room temperature. To initiate hemolysis, 0.5 mL of  $\text{H}_2\text{O}_2$  solution was added to each mixture. After incubating at 37°C for 1 h, the reaction mixtures were centrifuged for 10 min, and the percentage of hemolytic activity, corresponding to the liberation of hemoglobin due to hemolysis, was calculated using the following equation:

$$\text{Hemolytic activity} = \frac{AS - AN}{AP - AN} \times 100$$

Where AS is the absorbance of the sample, AN is the absorbance of the negative control (PBS) and

AP is the absorbance of the positive control ( $\text{H}_2\text{O}_2$ ).

#### Cytotoxicity Assay Using LDH

The lactate dehydrogenase (LDH) colorimetric activity test is a method used for evaluating cytotoxicity. This assay measures the activity of lactate dehydrogenase, an enzyme found in the cytosol, which is released when there is membrane damage or cell lysis. The LDH assay kit (Cytotoxicity) ab 65393 is utilized for this purpose.

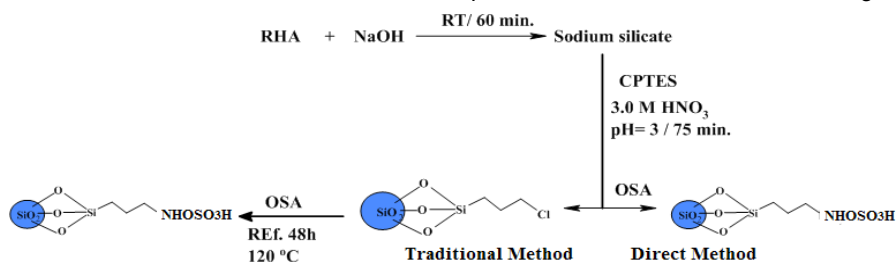
To perform the test, 0.5 mL of blood is collected, and plasma is separated through external centrifugation. Next, 100  $\mu\text{L}$  of the test sample is added, and 45  $\mu\text{L}$  of each sample is analyzed using an automatic clinical chemistry analyzer, specifically the FUJIFILM NX500 DRY CHEMISTRY model, over a duration of 5 minutes.

#### Statistical analysis

*In vitro* and other parametric all assays were performed in triplicates and results are expressed as mean $\pm$ SD.

## RESULTS AND DISCUSSION.

In both methods, silica was functionalized to have 3-chloropropyl end groups ( $-\text{Si}-\text{CH}_2\text{CH}_2\text{CH}_2\text{Cl}$ ) on its surface. The chloride in the 3-chloropropyl end groups was then replaced by OSA to yield ( $-\text{Si}-(\text{CH}_2)_3\text{NHOSO}_3\text{H}$ ), resulting in a catalyst with the same physical and chemical properties as shown in Scheme 1. Compared to traditional methods, the direct method is time-saving, uses more environmentally friendly solvents, has fewer steps in the synthesis, and achieves a higher yield of catalyst. Several techniques were employed to confirm the structure of the catalyst and its physical parameters, as detailed in the following subsections.



Scheme 1. The reaction bath for converted of sodium silicate to Si@OSA-Dir in direct method and Si@OSA-ref in reflux method

#### Elemental analysis

Elemental analysis of ash (RHA) and RHACCl indicated an increase in carbon content,

as shown in Table 1. After the incorporation of OSA onto RHACCl, the carbon levels in both catalysts, Si@OSA-ref and Si@OSA-Dir, were found to be

higher than those in either ash or RHACCI alone. Additionally, nitrogen and sulfur were detected in Si@OSA-ref and Si@OSA-Dir, while neither ash RHA nor RHACCI exhibited these elements. This finding confirms that OSA was successfully incorporated into silica through both methods.

**Table 1: Elemental analysis data of RHA and RHACCI, Si@OSA-ref and Si@OSA-Dir. The results were recorded beside EDX**

Catalyst	C	Elemental data (%)			
		Si	O	S	N
RHA [6]	9.9	37.6	51.1	0	0
RHACCI [6]	10.6	35.9	50.8	0	0
RHA@OSA-Dir	31.3	35.7	25.5	3.7	3.5
RHA@OSA-Ref	26.9	34.9	28.6	6.1	3.3

### X-ray Diffraction

The XRD diffraction patterns of Si@OSA-ref and Si@OSA-Dir are shown in Fig. 1 (a) and (b), respectively. Similar to the XRD diffraction pattern of ash reported previously<sup>18</sup>, both catalysts exhibit an amorphous nature, characterized by a single broad diffraction peak at an angle of 22.4 degrees ( $2\theta$ ). No sharp diffraction peaks were observed in the XRD

patterns. These results indicate that the surfaces of Si@OSA-ref and Si@OSA-Dir remained unchanged compared to the starting material (RHA) during the synthesis process.

### N<sub>2</sub> adsorption-desorption analysis

Figure 2 (a and b) presents the nitrogen adsorption-desorption isotherms along with pore size distribution graphs for Si@OSA-ref and Si@OSA-Dir, respectively. The isotherm appears to be of type IV, and the hysteresis loop resembles the H2 type, as determined within the range of  $0.3 < P/P_0 < 0.7$ , according to IUPAC classification<sup>17</sup>. Both Si@OSA-ref and Si@OSA-Dir exhibited the same specific surface area of 257 m<sup>2</sup>/g, with an average pore volume of 0.2216 cm<sup>3</sup>/g (see Table 2). This surface area is lower than that of the starting material, ash, and RHACCI<sup>6</sup>. The reduction in surface area may be attributed to the incorporation of OSA onto the silica surface. The pore size distributions for both catalysts are quite similar, falling within the micropore range, as they are less than 5 nm.

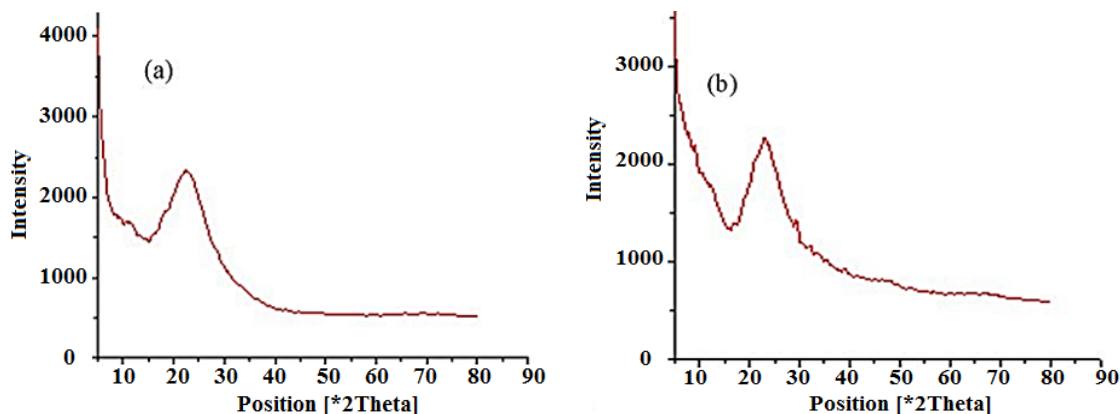


Fig. 1. The XRD of (a) Si@OSA-ref and (b) Si@OSA-Dir. An amorphous nature for both catalysts was recorded

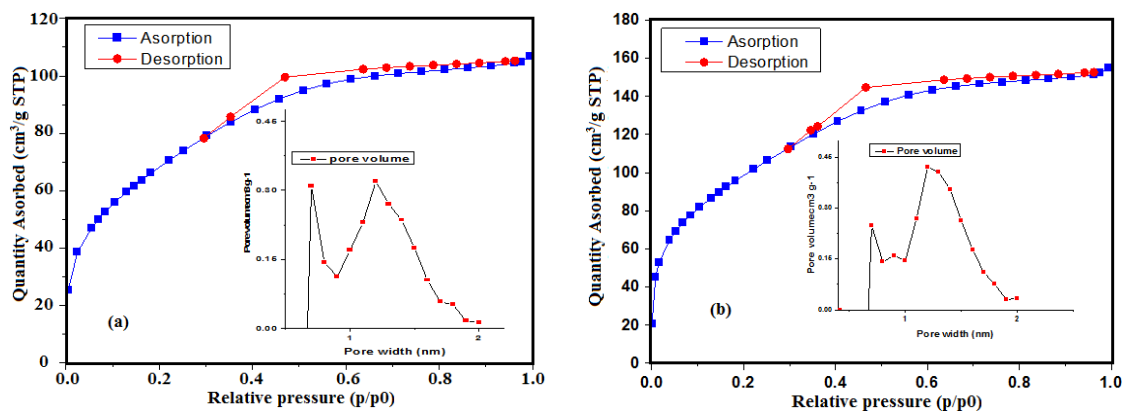


Fig. 2. The N<sub>2</sub> adsorption-desorption isotherms of (a) Si@OSA-Dir and (b) Si@OSA-ref with the corresponding pore size distribution inset

**Table 2: The specific surface area, average pore volume, and average pore diameter of RHA, RHACCI, and results Si@ OSA-Dir and Si@OSA-ref**

Sample	Specific surface area (m <sup>2</sup> g <sup>-1</sup> )	Average pore volume (cc g <sup>-1</sup> )	Average pore diameter(nm)
RHA [6]	347	0.87	10.4
RHACCI [6]	633	0.7	6.07
Si@OSA-Dir	257	0.15	1.2
Si@OSA-ref	257	0.22	1.2

### Thermal study

The TGA analysis of Si@OSA-Dir, shown in Fig. 3(a), clearly identifies three stages of decomposition. Moisture loss was observed between 40°C and 120°C, amounting to approximately 7%. The organic material loaded onto the silica began to decompose between 200°C and around 400°C, occurring in two distinct stages. The first stage likely corresponds to the loss of OSA, while the second stage is attributed to the loss of silane, specifically with CPTES. Overall, the total organic losses were found to be 18%. The remaining 5% mass loss observed from 500°C to about 900°C resulted from the loss of silanol groups on the silica surface.

In conjunction with the TGA results, the DTA revealed three exothermic transitions. The centers of these exothermic transitions occurred at 98°C, 230°C, and 446°C. The first exothermic transition is likely associated with moisture loss. The second and third transitions indicate significant decomposition, anticipated to be due to the loss of OSA and CPTES that were loaded onto the silica.

The TGA analysis of Si@OSA-ref is presented in Fig. 3(b). Similar to the previous catalyst, approximately 7% of moisture was lost between 30°C and 150°C. A further mass loss of 10% was observed between 200°C and 370°C, attributed to the thermal decomposition of organic compounds associated with OSA. Additionally, a third mass loss of 12% occurred between 400°C and 567°C, resulting from the loss of organic compounds that are directly bound to the silica surface, represented by the CPTES groups. A mass loss of 5% was noted between 639°C and 900°C due to internal changes on the silica surface, specifically the loss of the silanol group. The DTA curve indicates that an exothermic transition took place at 96°C due to moisture loss. The second and third exothermic transitions occurred

between 200°C and 250°C and 400°C and 450°C, respectively, indicating the decomposition of the organic components.

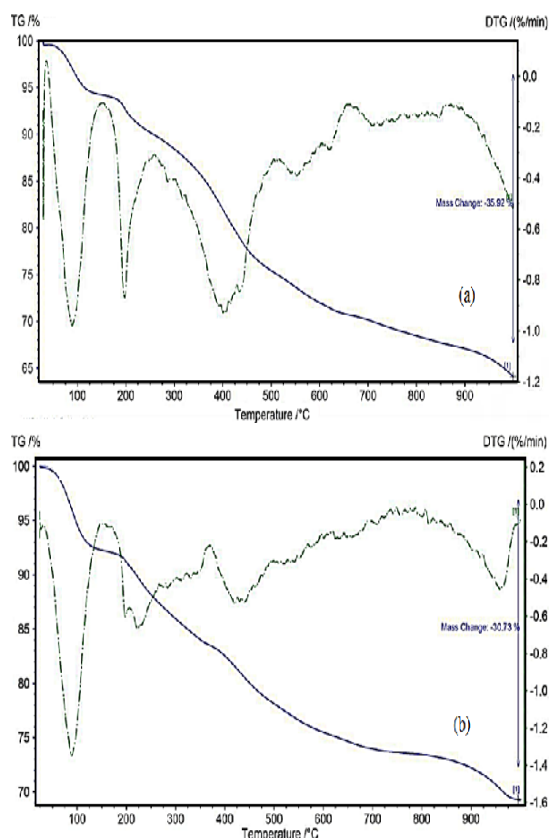


**Fig. 3. TGA/DTA curves of (a) Si@OSA-Dir, and (b) Si@OSA-ref**

### Scanning electron microscopy

The SEM images of Si@OSA-Dir are displayed in Fig. 4 (a, b). The surfaces exhibit a highly rough and porous texture with granular particles. These particles are spherical and tend to clump together, forming larger aggregates with a diameter ranging from 11 to 20 nm. There is no organized arrangement observed in these particles. In contrast, the SEM image of Si@OSA-ref, shown in Fig. 4 (c, d), reveals a very rough surface with smaller aggregates, but again, no organized arrangement is noted.

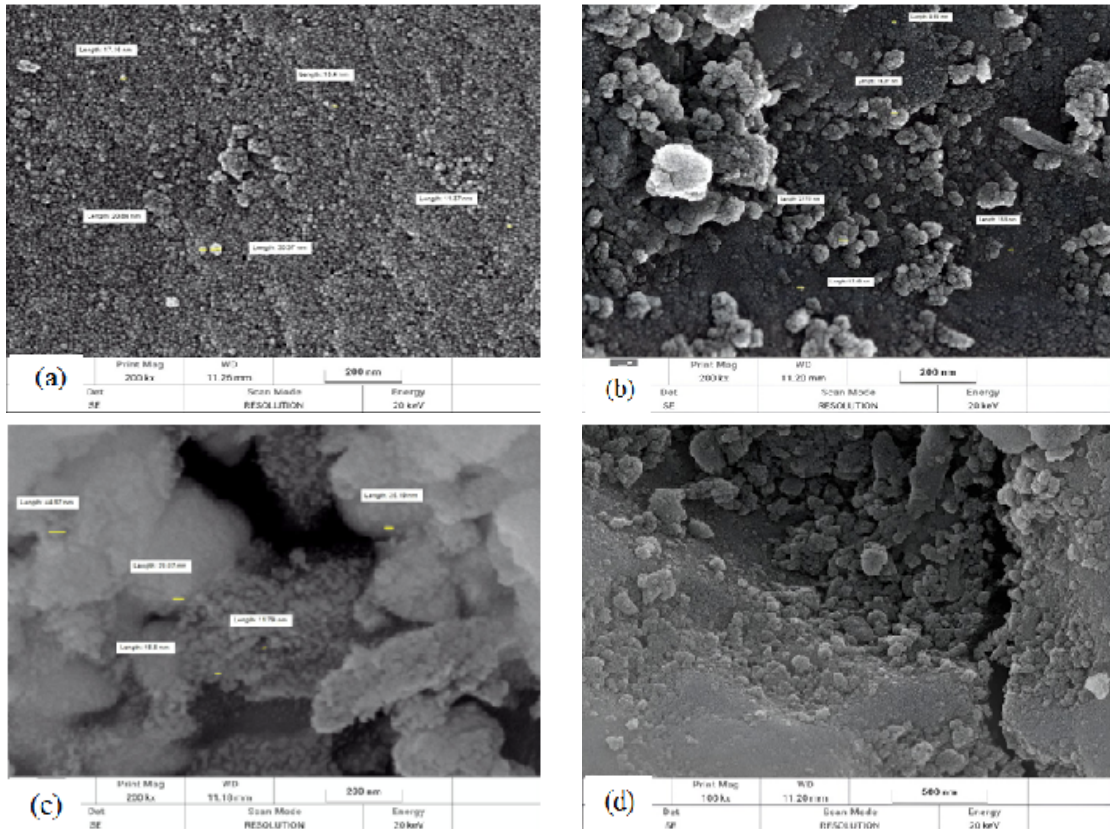


Fig. 4. The SEM images of (a, b) Si@OSA-Dir and (c, d) Si@OSA-ref at different magnification

### Transmission electron microscopy

Figure 5(a) displays a transmission electron microscope (TEM) image of Si@OSA-Dir. In this image, particles of irregular sizes, shapes, and diameters are randomly scattered across a porous surface. Some aggregates are clustered together and do not mix with

other aggregates, while others appear to be porous and share similar shapes. In Fig. 5(b), the TEM image of Si@OSA-ref shows that the particles in this sample are grouped together. No distinct shapes were identified. As illustrated in Fig. 5(b), several particles are situated close to one another.

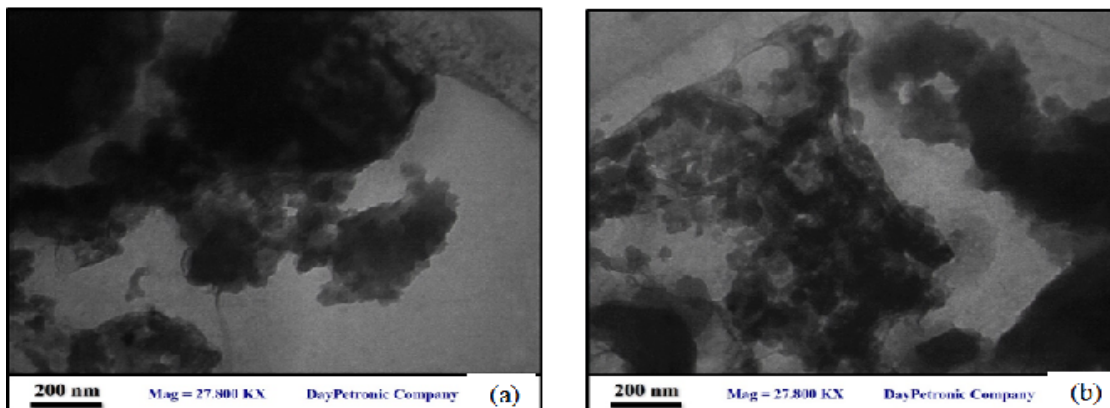


Fig. 5. The TEM micrographs of the (a) Si@OSA-Dir, and (b) Si@OSA-ref

### Hydrogen peroxide radical scavenging activity

The natural decomposition of hydrogen peroxide ( $H_2O_2$ ) leads to the formation of oxygen

and water, which can potentially generate hydroxyl radicals ( $\bullet OH$ )<sup>18</sup>. These radicals have the ability to initiate lipid peroxidation and cause DNA damage<sup>19</sup>.

In this context, we evaluated the effectiveness of silica (RHA) and Si@OSA-Dir and Si@OSA-ref in removing hydrogen peroxide. The capabilities of these catalysts to scavenge hydrogen peroxide are illustrated in Fig. 6. The catalysts Si@OSA-Dir and Si@OSA-ref demonstrated significant antioxidant potential. Both exhibited effective scavenging capacity against hydrogen peroxide. At a low concentration of 100  $\mu\text{g/mL}$ , Si@OSA-Dir and Si@OSA-ref showed inhibitory activities of 66.33% and 65.2%, respectively. At a low concentration the activity of the catalysts is very low due to the low number of active sites in the catalysts. Besides, the catalysts are heterogenous, and the active sites immobilized onto silica are expected to be very few, which led to a reduction in the activity of the catalysts. The highest percentage of scavenging activity, 90.3%, was observed at a concentration of 500  $\mu\text{g/mL}$ , compared to vitamin C, which used as the standard with a percentage inhibition of 93.0% (Fig. 6). These results suggest that the activity of these catalysts is due to their ability to donate electrons to hydrogen peroxide, thereby accelerating its neutralization into water. Consequently, the removal of  $\text{H}_2\text{O}_2$  is crucial for protecting pharmaceutical systems.

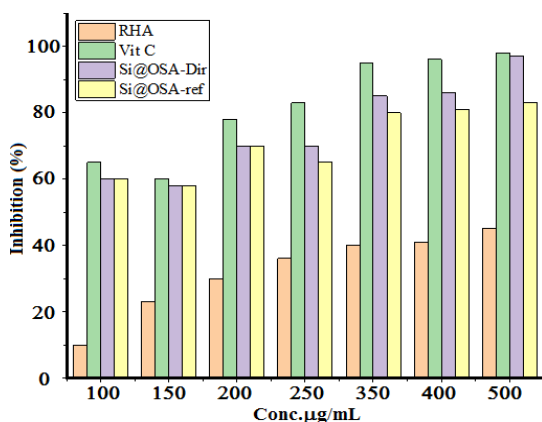


Fig. 6. Percentage inhibition of hydrogen peroxide scavenging activity of RHA, Si@OSA-Dir, and Si@OSA-ref in comparison to ascorbic acid

### Hemolytic Study

The extent of hemolysis appeared to be much more massive, during red blood cells exposure to any toxicant such as hydrogen peroxide. This study aimed to investigate whether Si@OSA-ref and Si@OSA-Dir inhibited and prevented injuries in the erythrocyte membrane or not. It was found that both catalysts showed minimal cytotoxicity at low concentrations of 100–150  $\mu\text{g/mL}$  in comparison to the positive control ( $\text{H}_2\text{O}_2$ ) which induced significant full hemolysis as in Fig. 7. On the other hand, when

cells were pre-treated with Si@OSA-Dir and Si@OSA-ref and then exposed to  $\text{H}_2\text{O}_2$ , cell viability rate remarkably raised as shown in Fig. 7 below which suggests they have antioxidants that protect hemolysis cells against  $\text{H}_2\text{O}_2$ . Fig. 8 (a,b and c) shows photos of the human blood smears examined by light microscopy illustration. Fig. 8(a) shows the normal red blood cells structure, while Fig. 8(b) for erythrocytes treated with the catalyst in presence of  $\text{H}_2\text{O}_2$  and Fig. 8(c) shows the decomposition of erythrocytes treated with  $\text{H}_2\text{O}_2$ . The normal shape of the erythrocytes appeared to provide key information for such compounds that may treat hemolytic diseases<sup>16</sup>. In addition, these promising compounds have the ability as potent antioxidants to protect RBCs from oxidative damage.

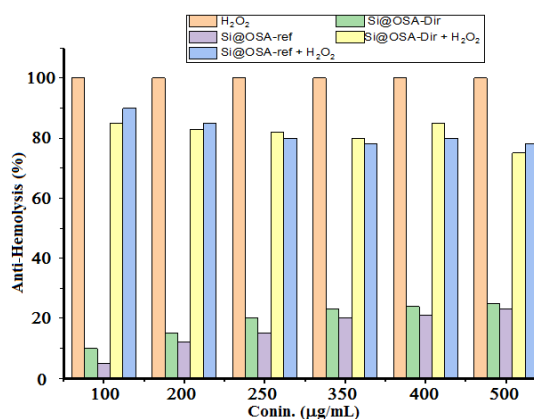


Fig. 7. Anti-hemolytic activity of Si@OSA-Dir, Si@OSA-ref against  $\text{H}_2\text{O}_2$  induced hemolysis phosphate buffer saline results in 0% hemolysis, hydrogen peroxide replaced extract to serve as a negative control since this treatment results in 100% hemolysis

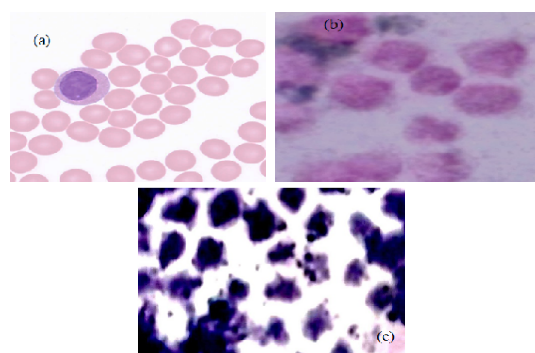


Fig. 8. Photos of erythrocytes at 100 X, (a) show normal, healthy erythrocytes suspended in Phosphate Buffered Saline (PBS), which is a common solution used for maintaining cell viability. (b) show cells exposed to Si@OSA (a silicon-based compound) and hydrogen peroxide ( $\text{H}_2\text{O}_2$ ), which is known to cause oxidative stress. (c) show cells exposed only to hydrogen peroxide ( $\text{H}_2\text{O}_2$ ), which is also known to cause oxidative stress

### Cytotoxicity Assay Using LDH

The LDH enzyme test is a common method used to detect hemolysis, which is the breakdown of red blood cells. When red blood cells break down, they release their contents, including lactate dehydrogenase (LDH), into the bloodstream, leading to elevated LDH levels<sup>19</sup>. In this study, the LDH enzyme test was performed to assess the potential for erythrocyte hemolysis in the presence of the Si@OSA-Dir and Si@OSA-ref catalysts. The results are illustrated in Fig. 9. A normal LDH level of 220 U/L was observed in the sample without any additives, serving as the baseline for comparison. When hydrogen peroxide was introduced, the LDH level increased significantly to 774 U/L, indicating that hydrogen peroxide caused considerable breakdown of red blood cells and ruptured cell membranes, resulting in the release of large amounts of LDH. This finding aligns with the established understanding that hydrogen peroxide is a powerful oxidant that damages cell membranes. In tests with the Si@OSA-ref and Si@OSA-ref samples, LDH levels of 148 U/L and 168 U/L were recorded, respectively. These lower levels compared to the normal range suggest that neither catalyst caused significant hemolysis and may provide protection to the cells. Furthermore, when hydrogen peroxide was used in the presence of both catalysts, the LDH levels decreased (to 554 U/L and 569 U/L, respectively). This reduction may indicate that the catalysts offer a partial protective effect against hydrogen peroxide-induced hemolysis.

The observed decrease in LDH activity following the addition of test samples can be attributed to two main factors. First, the presence of antioxidant components may help protect cells from lysis. For instance, if the sample contains electron-donating compounds, such as -OH or -NH<sub>2</sub> groups, these can mitigate the harmful effects of hydrogen peroxide. As a result, there is a reduced release of LDH. Second, the effect may stem from structural similarities between the sample components and cellular molecules. The sample could contain substances that interact similarly to cell proteins or membrane lipids, binding to hydrogen peroxide and thereby reducing its interaction with the cell membrane. This suggests that the sample functions

as a protective barrier or a reactive competitor, preventing hydrogen peroxide from directly attacking the cells.

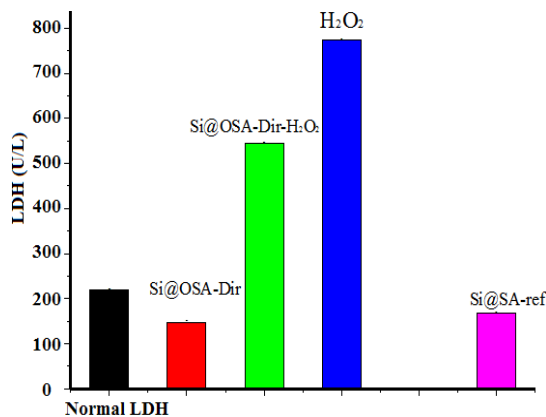


Fig. 9. Serum from different individuals exhibits different levels of LDH values as a marker of intravascular hemolysis activity in samples treated with the catalysts Si@OSA-Dir, Si@OSA-ref compared to H<sub>2</sub>O<sub>2</sub>. Elevated LDH can indicate red blood cell rupture and the release of its contents into the bloodstream (hemolysis)

### CONCLUSION

Using both direct and reflux methods, the OSA was successfully uploaded onto silica, producing two catalysts with the names Si@OSA-Dir and Si@OSA-ref. Carbon, Sulfur, and Nitrogen have been incorporated into the silica, according to elemental data analysis. The specific surface area of both catalysts was roughly 257 m<sup>2</sup>/g. At temperatures as high as 200°C, they showed stability. It was determined that Si@OSA-Dir and Si@OSA-ref were efficient catalysts that could be used to treat hemolytic illnesses. Furthermore, these encouraging findings owing to their unique physicochemical properties imply that both catalysts might serve as novel antioxidants for the treatment of oxidative stress, protecting red blood cells from damage.

### ACKNOWLEDGMENT

The work was supported by Al-Muthanna University, Republic of Iraq, for which the authors are grateful.

### Conflict of interest

The author declare that we have no conflict of interest.

## REFERENCES

1. Lin Y.-S.; Hurley K. R., *J. Phys. Chem. Lett.*, **2012**, *3*, 364–374.
2. Liu B.; Li C.; Cheng Z.; Hou Z.; Huang S.; Lin J., *Biomater. Sci.*, **2016**, *4*, 890–909.
3. Wang Y.; Zhao Q.; Han N.; Bai L.; Li J.; Liu J.; Che E.; Hu L.; Zhang Q.; Jiang T., *Nanomedicine.*, **2015**, *11*, 313–327.
4. Kumari B.; Singh D., *Ecol. Eng.*, **2016**, *97*, 98–105.
5. Chen H.; Wang W.; Martin J. C.; Oliphant A. J.; Doerr P.A.; Xu J. F.; DeBorn K. M.; Chen C., Sun L., *Chem. Eng.*, **2013**, *1*, 254–259.
6. Adam F.; Osman H.; and Hello K. M., *J. Colloid Interface Sci.*, **2009**, *331*(1), 143–147.
7. Hasan D. M.; Saoudi M. H., and Hello K. M., *AIP Conf. Proc.*, **2022**, 2398.
8. Zuwaid H. A. B., and Hello K. M., *Clean. Eng. Technol.*, **2023**, *16*, 100673.
9. Lippi G.; Blanckaert N.; Bonini P.; Green S.; Kitchen S.; Palicka V.; Vassault A. J.; Plebani M., *Clin. Chem. Lab. Med.*, **2008**, *46*, 764–772.
10. Marques-Garcia F., *EJFICC.*, **2020**, *31*, 85–97.
11. Zou J.; Nolan D.K.; LaFiore A.R.; Scott M.G., *Clin. Chim. Acta.*, **2013**, *421*, 60–61.
12. F. Adam and J.-H. Chua., *J Colloid Interface Sci.*, **2004**, *280*(1), 55–61.
13. A. E. Ahmed and F. Adam., *Microporous Mesoporous Mater.*, **2007**, *103*(1–3), 284–295.
14. M. M. Gaspar.; S Calado.; J Pereira.; H Ferronha.; I Correia.; H Castro.; AM Tomás.; MEM Cruz., *Nanomedicine: Nanotechnology, Biol. Med. Nanom. Nanotechnol.*, **2015**, *11*(7), 1851–1860.
15. M. Nave.; R. E. Castro.; C. M. Rodrigues.; A. Casini.; G. Soveral, and M. M. Gaspar., *Nanomedicine.*, **2016**, *11*(14), 1817–1830.
16. N. S. M. Vieira.; A. L. S. Oliveira.; J. M. M. Araújo.; M. M. Gaspar, and A. B. Pereiro., *Sustain. Chem.*, **2021**, *2*(1), 115–126.
17. F. Adam, S. Balakrishnan, and P.-L. Wong., *J. Phys. Sci.*, **2006**, *17*, 2, 1–13.
18. M. A. Ebrahimzad, S. F. Nabavi, and S. M. Nabavi, *Pakistan J. Biol. Sci.*, **2009**, *12*(5), 447–450.
19. A. Naqinezhad.; S. M. Nabavi.; S. F. Nabavi.; and M. A. Ebrahimzadeh., *Eur. Rev. Med. Pharmacol. Sci.*, **2012**, *16*(3), 88–94.